Dielectric function models for describing the optical properties of hexagonal GaN

Aleksandra B. Djurišić and E. Herbert Li[a]

Department of Electrical and Electronic Engineering, University of Hong Kong, Pokfulam Road, Hong Kong

Several different models have been employed for modeling the dielectric function of hexagonal GaN in the range from 1 to 10 eV. Models are compared in terms of number of parameters required, intricacy of model equations, and possibility of accurate estimation of important physical parameters, such as energies of critical points and exciton binding energies. Shortcomings and advantages of each model are discussed in detail. Excellent agreement with the experimental data for GaN has been achieved with three of the investigated models. It has also been shown that an assumption of adjustable broadening instead of a purely Lorentzian one improves the agreement with the experimental data and enables elimination of excessive absorption below the gap which is inherent to the models with Lorentzian broadening. © *2001 American Institute of Physics.* [DOI: 10.1063/1.1331069]

I. INTRODUCTION

Group-III nitrides have recently attracted lots of interest because of their potential applications in optoelectronic devices operating in the visible and ultraviolet region.[1,2] Group-III nitrides are characterized by high ionicity, very short bond lengths, low compressibility, and high thermal conductivity. Fundamental band gaps of InN, GaN, and AlN are around 1.9, 3.5, and 6.2 eV, respectively, enabling their ternary alloys to have band gaps in spectral regions from orange to ultraviolet. A number of devices based on group-III nitrides has been developed, such as light-emitting and laser diodes, ultraviolet sensors, optical pumping structures, photodetectors, and heterostructure field effect transistors.

Optical response of material is usually described in terms of the optical functions such as the complex dielectric function $\epsilon(\omega) = \epsilon_1(\omega) + i\epsilon_2(\omega)$ or the complex index of refraction $N(\omega) = n[(\omega) + ik(\omega)]$. Optical functions values can be determined experimentally, where measured quantities differ for different experimental methods. Optical functions are usually derived from spectroscopic ellipsometry (SE) or reflectance measurements, although some other techniques such as electron-energy-loss spectroscopy can also be used. However, the experimental dielectric function is not expressed as an analytical function of the photon energy $E = \hbar\omega$. Fitting the experimental data to a suitable model enables overcoming this deficiency. Modeling the dielectric function is useful in the quantitative interpretation of the measured optical spectra, especially if the films of interest are contained within a complex multilayer structure. This is generally the case for nitride materials, since for the accurate derivation of the optical functions one has to take into account the substrate, buffer layer (if any), nitride film, and oxide overlayer. Also, surface roughness should be adequately modeled. Modeling is also useful in monitoring and control during the growth of the films. Some models also enable determination of the important material parameters such as critical point energies and exciton binding energy.

The imaginary part of the dielectric function can be calculated using a strict quantum mechanical approach, while the real part is obtained through Kramers–Kronig (KK) transformation. This approach is straightforward and has been applied for calculating the dielectric function of GaN.[3–7] However, such an approach as a rule produces too sharp and pronounced peaks in the dielectric function. Recently, *ab initio* or first principle calculations which take into account excitonic effects, i.e., electron-hole interaction, have been reported for several materials (diamond, Si, Ge, and GaAs;[8] LiF and MgO;[9] GaAs and LiF;[10] Si[11], GaN and CaF$_2$).[12] It has been shown that the agreement with the experimental data is improved compared with the traditional approach which does not take into account electron-hole interactions. However, there still exists large discrepancies between the calculated and experimental data so that such an approach cannot be used for describing accurately the optical functions. In addition, careful interpretation of the position and magnitude of the calculated peaks is needed since there may exist structures which are absent in the experimental data.[13] This effect has been attributed to the choice and number of k points in the Brillouin zone sampling.[14]

In this work we employ several different semi-empirical models for modeling the dielectric function of GaN. The purpose of this is twofold. First, we want to examine in detail the advantages and shortcomings of each model and provide guidance to which of the models should be employed depending on the requirements imposed. Second, we want to provide sets of model parameters which would enable easy and accurate calculations of the dielectric function of GaN, which could be readily applied in the optoelectronic device design. In the latter case, it is necessary to carefully choose the set of experimental data used for the model parameter estimation. The optical functions data for GaN reported in
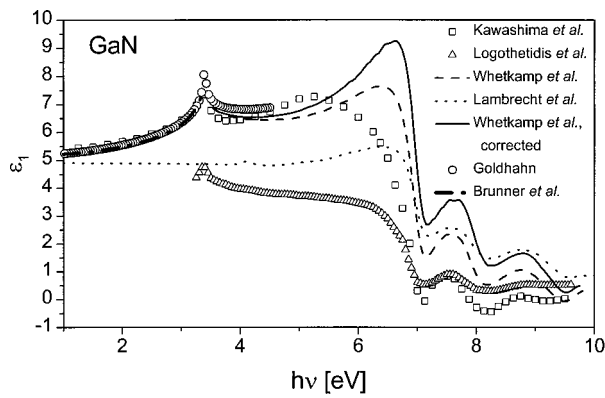
[a]Electronic mail: ehli@eee.hku.hk

273

FIG. 1. The real part of the dielectric function of GaN. The dashed line denotes SE data by Whetkamp et al. (see Ref. 15) the solid line represents Whetkamp et al.'s data corrected for the surface roughness (Ref. 16) the circles denote the data measured by Goldhahn (see Ref. 16) the triangles are the SE data by Logothetidis et al. (see Ref. 17) the squares are the data of Kawashima et al. (see Ref. 18) who performed surface roughness correction over the data of Logothetidis et al. (see Ref. 17) and the dotted line denotes the reflectance data of Lambrecht et al. (see Ref. 5).

the literature widely differ among themselves. This is illustrated in Figs. 1 and 2, depicting the available experimental data for the real and imaginary part of the dielectric function, respectively. The dashed line denotes SE data by Whetkamp et al.,[15] the solid line represents Whetkamp et al.'s data corrected for the surface roughness,[16] the circles denote the data measured by Goldhahn,[16] the triangles are the SE data by Logothetidis et al.,[17] the squares are the data of Kawashima et al.[18] who performed surface roughness correction over the data of Logothetidis et al.,[17] the dotted line denotes the reflectance data of Lambrecht et al.,[5] and the dash-dot line is ϵ_1 data calculated from the expression of Brunner et al.[19] In general, the optical functions data derived by performing the KK transformation over the normal incidence reflectance data can be considered less accurate than the SE data. It can be observed that the data of Lambrecht et al.[5] are inferior to the SE data, according to criterion of Aspnes and Studna.[20]
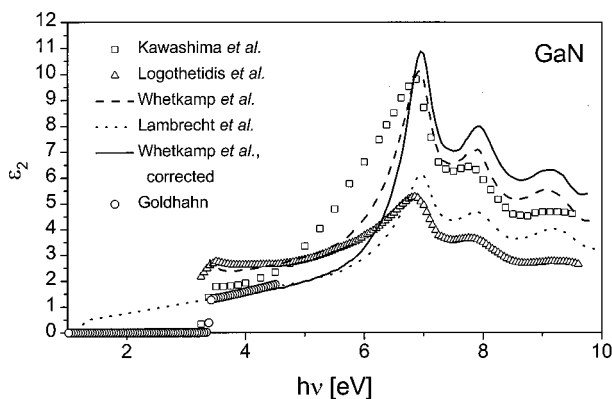

FIG. 2. The imaginary part of the dielectric function of GaN. The dashed line denotes SE data by Whetkamp et al. (see Ref. 15) the solid line represents Whetkamp et al.'s data corrected for the surface roughness (see Ref. 16) the circles denote the data measured by Goldhahn (see Ref. 16) the triangles are the SE data by Logothetidis et al. (see Ref. 17) the squares are the data of Kawashima et al. (see Ref. 18) who performed surface roughness correction over the data of Logothetidis et al. (see Ref. 17) and the dotted line denotes the reflectance data of Lambrecht et al. (see Ref. 5).

However, reflectivity studies can still be a useful tool for the determination of the optical functions of GaN, as demonstrated by Shokhovets et al.[21] and Goldhahn et al.[22] It has been shown that the influence of a buffer layer and/or a nonabrupt substrate/film interface can be verified by analyzing the envelopes of the reflectivity spectrum.[21,22] Significant influence of the surface roughness to the determined values of the optical functions can be clearly observed in Fig. 1, where the data with surface roughness correction show larger peaks in ϵ_2. It has been shown that a low temperature buffer layer should be deposited first in order to grow good quality nitride films free of cracks.[23,24] It has also been shown that samples grown by metalorganic chemical vapor deposition have more abrupt surfaces than molecular beam epitaxy grown ones.[15] The surface abruptness of nitride films can be further improved by wet chemical treatments.[25] For an accurate determination of the optical constants, an appropriate three- or four-layer model should be adopted, which can take into account the substrate, buffer layer (if any), nitride film, and overlayer/surface roughness effects (if they are not chemically removed). Since hexagonal GaN films are usually grown on either sapphire or 6H-SiC substrates, which are transparent in the most interesting region, i.e., around the fundamental band gap of GaN, it is also necessary to take into account incoherent reflections from the backside of the substrate. Influence of the errors due to disregarding this effect to the accuracy of reflectance spectroscopy has been analyzed in details,[26] and appropriate corrections for both reflectance measurements[27,28] and spectroscopic ellipsometry[29] have been proposed. Also, one should have in mind that the hexagonal materials are essentially anisotropic. The refractive index of GaN for both polarization directions has been measured by Goldhahn et al.[22] and Bergmann et al.,[30] and it has been found that both the ordinary ($E\perp c$) and extraordinary ($E\|c$) refractive indices are higher than the isotropic one.

Taking into consideration the method employed for the determination of the optical functions and the criterion of Aspnes and Studna,[20] we have chosen to fit the data consisting of the data of Goldhahn[16,22] in the range from 1 to 4.5 eV and the data of Whetkamp et al. corrected for the surface roughness[16] in the range 5.8–10 eV. We have decided to disregard the data of Whetkamp et al.[15,16] below 5.8 eV since the data do not join smoothly with the data of Goldhahn[16,22] and accuracy of Whetkamp et al.'s[15] data below 6 eV may be lower. Since Goldhahn's data[16] have been determined from a combination of SE and reflectance study using a multilayer sample model, those data in the vicinity of the band gap and below should be more accurate than the data of Whetkamp et al.[15] Unfortunately, the SE data above 6 eV (the upper limit of commercial ellipsometers) are scarce. For detailed review of SE in the 6–35 eV range see Ref. 31.

The article is organized as follows. In the following section, description of the investigated models is given. In Sec. III advantages and shortcomings of each model are discussed in terms of the agreement with the experimental data, intricacy of the model equations, number of parameters required, and their physical meaning. Finally, conclusions are drawn.

II. DIELECTRIC FUNCTION MODELS

We will describe several semi-empirical models which can be used for describing the optical constants of hexagonal GaN in the spectral region from 1 to 10 eV.

A. Damped harmonic oscillator model

The damped harmonic oscillator (DHO) model is a simple model which can achieve excellent agreement with the experimental dielectric function data, depending on the number of oscillators (the general rule is: more oscillators, better fit). However, the DHO is not appropriate for the description of the derivatives of the dielectric function,[32] and its parameters are not directly related to the band structure. Usually, oscillator energy is close to the energy of a critical point (CP), but often a number of oscillators needed to describe single transition is larger than one, and some additional oscillators between CPs may be needed. This model has low accuracy in the vicinity of the fundamental band gap, since the line shape of the $\epsilon_2(\omega)$ cannot be successfully described with the sum of Lorentzian peaks.[32] According to the DHO model, dielectric function is given by[33]

$$\epsilon(E) = 1 - \sum_{j=1}^{N} A_j \left(\frac{1}{E + E_j + i\Gamma_j} - \frac{1}{E - E_j + i\Gamma_j} \right), \quad (1)$$

where $E = \hbar\omega$ is the photon energy, Γ_j is the damping constant, A_j is the strength, and $E_j = \hbar\omega_j$ is the oscillator energy. Phenomenological linewidths Γ_j in this model have no relationship with true linewidths and are usually much larger.[32] Terry[34] has proposed a modification of this model by allowing the strengths A_j to be complex numbers $A_j = |A_j| \times \exp(i\phi_j)$ which significantly improved the accuracy of the model. However, the number of required parameters is quite large. Terry[34] used nine oscillators (36 parameters for one sample, 144 for the entire alloy range) for describing the dielectric function of $Al_xGa_{1-x}As$ in the 1.5–6.0 eV range. The accuracy of the DHO model can be improved with the use of adjustable broadening,[35] which will be described in details in the following. In this work we have used the following expression for the DHO dielectric function:[35]

$$\epsilon(\omega) = \epsilon_{1\infty} + \sum_{j=1}^{N} \frac{F_j}{\omega^2 - \omega_j^2 - i\omega\Gamma_j}, \quad (2)$$

where $F_j = f_j\omega_j^2$ is the parameter associated with the oscillator strength f_j, and $\epsilon_{1\infty}$ is the dielectric constant arising from the higher-lying transitions. No previous attempts to model the optical constants of nitride materials using the DHO model have been reported. There have been attempts to model the refractive index of hexagonal[36] and zinc-blende[37] GaN using Sellmier equation $n^2(\lambda) = A + B/(\lambda^2 - C)$ but this is valid only in the transparent spectral region. In principle, the DHO model can be applied to a wide variety of materials, unquestionably including group-III nitrides. The main shortcomings of the model are: low accuracy in the vicinity of the absorption edge, large number of parameters required to achieve higher accuracy, little or no information on the band structure parameters can be derived from the model, and the model is not appropriate for the description of the derivatives of the dielectric function.[32] The main advan-

tage is extreme simplicity of the model equation. Reasonably accurate approximation of the dielectric function can be achieved if sufficient number of oscillators is used.

B. Model of Forouhi and Bloomer

The model of Forouhi and Bloomer (MFB)[38,39] is another simple model which can be applied to a variety of materials, although no application to group-III nitrides have been reported. This model has similar characteristics as the DHO, despite the fact that it is based on the quantum mechanical theory of absorption. Only parameter related to the electronic band structure is the band gap E_0, which is generally underestimated. Like the DHO model, the MFB is not appropriate for the description of the derivatives of the dielectric function and has low accuracy in the vicinity of the band gap, with refractive index underestimated below the gap. However, the MFB requires fewer parameters than the DHO, (usually only 14) In the MFB, extinction coefficient is given by[38,39]

$$k(E) = \left[\sum_{i=1}^{q} \frac{A_i}{E^2 - B_iE + C_i} \right](E - E_0)^2, \quad (3)$$

where A_i, B_i, and C_i are adjustable parameters, E_0 is the band gap, and q is the number of transitions (usually $q = 4$) The refractive index is given by[38,39]

$$n(E) = n(\infty) + \sum_{i=1}^{q} \frac{B_{0i}E + C_{0i}}{E^2 - B_iE + C_i}, \quad (4)$$

where

$$B_{0i} = \frac{A_i}{Q_i}(-B_i^2/2 + E_0B_i - E_0^2 + C_i), \quad (5)$$

$$C_{0i} = \frac{A_i}{Q_i}[(E_0^2 + C_i)B_i^2/2 - 2E_0C_i], \quad (6)$$

$$Q_i = \tfrac{1}{2}\sqrt{4C_i - B_i^2}. \quad (7)$$

The main shortcoming of this model is low accuracy below E_0, where the refractive index is underestimated. Furthermore, k is not zero below the gap, and the band gap value E_0 is also underestimated. Other parameters in the band structure cannot be estimated. Advantages of the MFB are simplicity of the model equations and low number of parameters required. A modification of this model has been proposed by Chen et al.[40] but this modification does not address shortcomings mentioned before. The modification proposed[40] provides that the model conforms with the symmetry relation and the f-sum rule for $k(\omega)$. Better agreement achieved for energies higher than 7 eV is most probably due to taking into account more transitions (11–14) where Forouhi and Bloomer[38,39] considered only 4 and fitted the data up to 7 eV. Other modifications of the MFB proposed in the literature which address the problem $k(E) > 0$ for $E < E_0$ deal with amorphous and not crystalline materials.[41,42]

C. Adachi's model

Adachi's model dielectric function (MDF) represents a relatively simple model which combines standard critical points (SCP) model and the DHO model. The SCP model[43,44] describes contributions of each critical point with expression

$$\epsilon(\omega) = C - A \exp(i\phi)(\hbar\omega - E + i\Gamma)^n, \tag{8}$$

where A is the amplitude, E is the energy threshold, Γ is the broadening, and ϕ is the excitonic phase angle. The exponent n has different values for different types of CPs. For one-dimensional CPs $n = -1/2$, for two-dimensional (2D) CPs $\ln(\hbar\omega - E + i\Gamma)$ is considered, and $n = 1/2$ for three-dimensional (3D) CPs. Discrete excitons with Lorentzian line shape are represented by $n = -1$. SCP provides an excellent fit to the second and third derivatives of the dielectric function, but gives only moderately good representation of the dielectric function itself.[32] It should be pointed out that in fitting the derivatives of the dielectric function one should use numerical derivatives for both the experimental data and the model,[45,46] instead of commonly used approach to fit the numerical derivatives of the experimental data with the analytical derivatives of the model. Ability for describing the derivatives of the dielectric function is necessary for modeling the electroreflectance and photoreflectance data. Also, critical point energies can be more accurately determined from fitting the derivative spectra. The SCP model has been frequently applied for the determination of positions of the critical points and their temperature dependence for several materials, including both cubic and hexagonal GaN.[17,47]

Brunner et al.[19] have used the SCP model for describing the refractive index of $Al_xGa_{1-x}N$, taking into account only transitions at E_0 in the form

$$n^2(\hbar\omega) = \epsilon(\hbar\omega)$$
$$= C(x) + A(x)y^{-2}[2 - (1+y)^{1/2} - (1-y)^{1/2}], \tag{9}$$

where $C(x) = -(2.2 \pm 0.2)x + (2.66 \pm 0.12)$, $A(x) = (3.17 \pm 0.39)\sqrt{(x + (9.98 \pm 0.27))}$, $y = \hbar\omega/E_0(x)$, and $E_0(x) = (6.13 - 3.42 \text{ eV})x + 3.42 \text{ eV}x - bx(1-x)$, and $b = 1.3$ eV. However, this expression is valid only below the band gap, where $y \leq 1$. In order to use it slightly above the band gap and also estimate the imaginary part of the index of refraction it is necessary to take into account that the dielectric function $\epsilon = \epsilon_1 + i\epsilon_2$ has a complex value, so that[48]

$$\epsilon_1(\hbar\omega) = \epsilon(\hbar\omega)$$
$$= C(x) + A(x)y^{-2}[2 - (1+y)^{1/2}$$
$$- (1-y)^{1/2}\Theta(1-y)], \tag{10}$$

and

$$\epsilon_2(\hbar\omega, x) = A(x)y^{-2}(y-1)^{1/2}\Theta(y-1), \tag{11}$$

where

$$\Theta(x) = \begin{cases} 1, & x \leq 0 \\ 0, & x < 0 \end{cases}. \tag{12}$$

The real and imaginary parts of the index of refraction are then calculated from $n = \{0.5[\epsilon_1 + (\epsilon_1^2 + \epsilon_2^2)^{1/2}]\}$ and $k = \{0.5[-\epsilon_1 + (\epsilon_1^2 + \epsilon_2^2)^{1/2}]\}$.

In Adachi's model for hexagonal materials,[18] contributions of the four lowest CPs ($E_0, E_{1\beta}, \beta = A, B, C$ for hexagonal materials) are taken into account. Additional damped harmonic oscillators for contributions of higher-lying critical points, indirect transitions, discrete excitons as well as recently proposed terms describing continuum excitons,[49] can be taken into account if needed. Since we limit our discussion to the wurtzite group-III nitrides, we will describe the MDF for hexagonal semiconductors. For the MDF equations for the semiconductors with zinc-blende structure, see Refs. 48 and 50.

For hexagonal materials, contribution of the fundamental band gap E_0 is given by[18]

$$\epsilon_0(E) = AE_0^{-3/2}\chi_0^{-2}[2 - (1+\chi_0)^{1/2} - (1-\chi_0)^{1/2}], \tag{13}$$

where

$$\chi_0 = \frac{E + i\Gamma_0}{E_0}, \tag{14}$$

while A and Γ_0 are the strength and damping constants of the E_0 transition, respectively. Normally, one should calculate the separate contributions from $E_{0\beta}, \beta = A, B, C$ critical points, but due to very small splitting energies among these critical points, $E_{0\beta}$ can be treated as a single degenerate one.[18]

Exciton contributions at E_0 critical points are given by[18]

$$\epsilon_{0X}(E) = \sum_{m=1}^{\infty} \frac{A_0^{\text{ex}}}{m^3} \frac{1}{E_0 - (G_0^{3D}/m^2) - E - i\Gamma_0}, \tag{15}$$

where A_0^{ex} is the 3D exciton strength parameter and G_0^{3D} is the 3D exciton binding energy.

$E_{1\beta}$ CPs are of 3D M_1 type, but since the longitudinal mass is much larger than the transverse one, they can be approximated by 2D M_0 type.[50,51] Contributions of the 2D M_0 critical points $E_{1\beta}$ are given by[18]

$$\epsilon_1(E) = -\sum_{\beta=A,B,C} B_{1\beta}\chi_{1\beta}^{-2} \ln(1 - \chi_{1\beta}^2), \tag{16}$$

where

$$\chi_{1\beta} = \frac{E + i\Gamma_{1\beta}}{E_{1\beta}}, \tag{17}$$

$B_{1\beta}$ and $\Gamma_{1\beta}$ are the strengths and damping constants of the $E_{1\beta}$ transitions, respectively.

Contributions of the Wannier type 2D excitons (discrete series of exciton lines at the $E_{1\beta}$ critical points are given by)[18]

$$\epsilon_{1X}(E) = \sum_{\beta=A,B,C} \sum_{m=1}^{\infty} \frac{B_{1\beta}^X}{(2m-1)^3}$$
$$\times \frac{1}{E_{1\beta} - [G_{1\beta}^{2D}/(2m-1)^2] - E - i\Gamma_{1\beta}}, \tag{18}$$

where $B_{1\beta}^X$ and $G_{1\beta}^{2D}$, are the strengths and binding energies of the excitons at $E_{1\beta}$, respectively. Total dielectric function is then given by $\epsilon(E) = \epsilon_{1\infty} + \epsilon_0(E) + \epsilon_{0X}(E) + \epsilon_1(E) + \epsilon_{1X}(E)$.

This model is relatively simple, but not very accurate especially around the fundamental absorption edge. Several modifications of the MDF for zinc-blende[52–55] and hexagonal[56,57] semiconductors have been proposed. The best improvement in the accuracy is obtained using an adjustable broadening concept.

The MDF has been employed for modeling the dielectric constant of hexagonal GaN,[18] but obtained agreement with the experimental data has been poor. It has been shown that the agreement with the experimental data for GaN can be improved by using the modified MDF with adjustable broadening.[56,57] Also, the improvement of accuracy of the conventional MDF is possible by taking into account one-electron contributions at $E_{1\beta}$ CPs and higher-order exciton contributions (which were disregarded in the study of Kawashima *et al.*[18]) and using a global optimization algorithm[58] for model parameter determination.[57] However, there exists an important problem in the application of this model. If no constraints are imposed on the values of exciton related model parameters, exciton binding energy is usually overestimated. Overestimation of the exciton related parameters in the Adachi's model has been attributed to the fact that the parameters for bound and unbound states are not independent.[59] Tanguy[59–61] has proposed an analytical expression which takes into account the contributions of all bound and unbound states in the vicinity of the absorption threshold. However, the proposed expression is rather intricate and its agreement with the experimental data has been verified only over a very narrow spectral region.[59,62] It should be pointed out that the low sensitivity of the objective function to the exciton related parameters, especially over a wide spectral range considered, represents additional difficulty for their accurate determination. We have tried to fit the derivatives of the dielectric function to obtain more accurate values of exciton binding energies, but in that case agreement with the dielectric function deteriorates. In case of simultaneous fitting of the dielectric function and its derivative(s), similar to the method proposed by Kim *et al.*,[32] it is difficult to achieve convergence. This might indicate that the model equations may not be appropriate for describing the dielectric function and its derivatives at the same time. The best method for dealing with this problem, in our experience, is to impose constraints on the exciton binding energies, or determine exciton related parameters from the narrow spectrum around the gap and then keep them fixed in the final fitting procedure. Agreement of the MDF with the experimental data can be improved with adjustable broadening modification, but the obtained exciton related parameters still give just a rough estimate of the value.

The problem of determination of exciton binding energy from the room temperature dielectric function data where exciton peaks are not clearly pronounced can be clearly understood from Fig. 3 depicting the calculated dielectric function for different exciton binding energy values G_0^{3D}. Small difference between the curves with higher values of the ex-
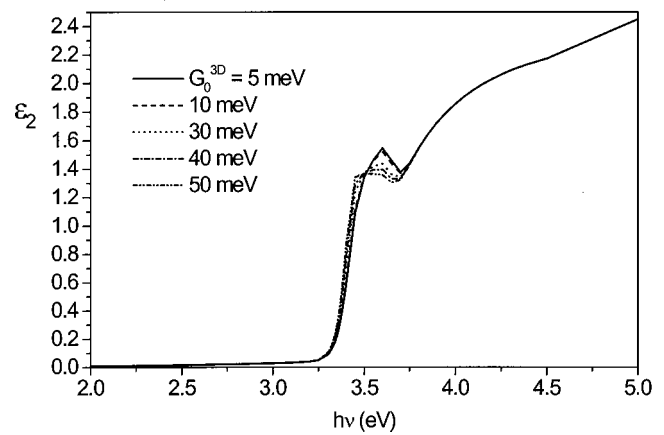

FIG. 3. The calculated imaginary part of the dielectric function for different values of exciton binding energy G_0^{3D}.

citon binding energy may explain the tendency of the model to overestimate the exciton binding energy value. Improvement of the estimate of the exciton related parameters may be achieved by enhancing the region in the vicinity of E_0 either with larger number of data points or with higher weight of those points, but this approach might cause deterioration of the accuracy outside the enhanced spectral region. The objective function is more sensitive to the changes of $G_{1\beta}^{2D}$ values. However, position of the peak corresponds to $E_{1\beta} - G_{1\beta}^{2D}$ values, and there exists a number of combinations of $(B_{1\beta}^X, E_{1\beta}, G_{1\beta}^{2D}, \Gamma_{1\beta})$ values which give similar dielectric function curves.

D. Adjustable broadening concept and modified critical points model

The accuracy of both the DHO and MDF can be improved if the adjustable broadening is introduced. Simple Lorentzian broadening, which is frequently used, does not represent accurate approximation of the lifetime broadening. effect[32,55,57,63–65] The Lorentzian function has wide wings, which give rise to the excessive absorption below the band gap. It has been shown that the Gaussian line shape yields better fits to the experimental data than the Lorentzian one in case of direct band gap binary semiconductors.[63] However, if a Gaussian broadening is assumed, the dielectric function cannot be expressed in a closed analytical form. In order to overcome this problem, Kim *et al.*[32,66–68] have replaced the damping constant Γ_i in their model with frequency dependent expression

$$\Gamma_i'(\omega) = \Gamma_i \exp\left[-\alpha_i\left(\frac{\hbar\omega - E_i}{\Gamma_i}\right)^2\right], \tag{19}$$

where E_i is the critical point energy, and α_i and Γ_i are model parameters. For the model of Kim *et al.*[32,66–68] $\alpha \approx 0.2$ approximates well the Gaussian broadening. They have investigated only two cases $\alpha = 0$ (Lorentzian broadening) and $\alpha \approx 0.2$ (Gaussian-like broadening). Better agreement with the experimental data for all the investigated materials has been achieved in the latter case. We will not discuss here the model of Kim *et al.*[32,66–68] in detail since the model equations are rather intricate, it requires large number of param-

eters, and up to date it has been applied over a wide spectral range only to zinc-blende materials. But it should be pointed out that this model gives excellent approximation of both the dielectric function and its first three derivatives. Effects of discrete excitons have also been incorporated in this model recently.[68]

It has been shown that improvement in the agreement with the experimental data can be achieved by replacing the damping constant Γ with Eq. (19) for the DHO model,[35] the MDF for zinc-blende materials,[55] and hexagonal materials.[56,57] In this work, we will model the optical functions of GaN with the modified DHO model with adjustable broadening (MDHO) and modified MDF with adjustable broadening (MMDF). In both cases, we simply replace the damping constants in model equations with frequency dependent expression and treat each α_i as an adjustable parameter. Similar changes in the shape of the dielectric function achieved by varying α/Γ ratio[57] can be obtained by a convolution of Lorentzian and Gaussian lines, which can be determined analytically in a closed form[65] or calculated numerically.[64] It has been shown that the room temperature dielectric function of binary compounds is approximately a linear combination of 75% Gaussian and 25% Lorentzian representations.[63] Since broadening is neither pure Gaussian nor pure Lorentzian, an adjustable broadening concept is necessary to deal with this problem. Fourier approach to the determination of the critical points energies and broadening parameters has been proposed.[69,70] It has been found that the broadening of $E_1, E_1 + \Delta_1$ transitions in CdTe is purely Lorentzian.[69] However, E_0 transition where inadequacy of the Lorentzian approximation in the form of extended absorption tail is most notable was not analyzed with this method. We have tried to apply the same approach to determine the type of broadening of E_0 for GaN. However, we have found that the dependence of the logarithm of Fourier coefficients $\log_{10} C_n$ on the order n is not independent on the false data (or the choice of boundaries outside which false data are used) and base line correction. Furthermore, results are dependent on the number of data points and the width of the spectral region considered not only for the experimental data, but also for a simple Lorentzian or Gaussian function. It has been shown that the accuracy of the broadening parameter Γ obtained by this method depends on how close the data are spaced in energy, and poor values can be obtained if the data spacing is larger than 0.4Γ.[46] Therefore, Fourier analysis method proposed by Aspnes[69,70] can be useful for the determination of the energies of the critical points but caution is needed in deriving any conclusions about broadening.

To summarize, models with adjustable broadening are very flexible, can deal with inhomogeneously broadened transitions, and can achieve excellent agreement with the experimental data. However, aside from the significant improvement in the accuracy of the approximation of the dielectric function, models with adjustable broadening have the same shortcomings as the models in which the broadening modification was introduced. Also, the number of parameters may be larger (one additional parameter per transition), but not necessarily since fewer terms can be used without

impairing the accuracy. Additional worry may be KK consistency of the model. However, our numerical checks revealed good agreement between the KK transformation of the imaginary part and model equations for the real part of the dielectric function. The real and imaginary part of a complex function are Hilbert transforms of one another if the function satisfies the conditions: (a) the function $\Phi(z), z = x + iy$ is analytical for $y > 0$ and (b) $(\exists K)(\forall y > 0) \int_{-\infty}^{+\infty} |\Phi(x + iy)|^2 dx < K$ for all values of y.[71] Simply replacing Γ with $\Gamma(\omega)$ given by Eq. (19) should not influence these conditions, and hence, should not cause KK inconsistency. Also, considered spectral range is not wide enough for this issue to be of consequence. Still, it is advisable to perform numerical checks of KK consistency when using the adjustable broadening concept, especially for large values of α.[72]

Let us describe the modified critical point model (MCP). The dielectric function within the parabolic approximation and for the Lorentzian representation[63] can be described with

$$\epsilon(E) = \epsilon_{1\infty} + \sum_{i=1}^{N} C_i (E - E_i + i\Gamma_i)^{-m_i}, \tag{20}$$

where C_i is a constant, E_i is the critical point energy, Γ_i is the damping constant, and $m_i = 1 - d/2$ where d is the dimension of the critical point [for $d = 2$, $\ln(E - E_i + i\Gamma_i)$ is considered in the standard critical points model]. A modification where $m_i, i = 1, N$ are treated as adjustable parameters achieves the similar effect as introducing Gaussian line shape.[63] The model is simple, does not require large number of parameters, and can achieve excellent agreement with the experimental data. However, as in the case of models with adjustable broadening, parameters Γ_i cannot be directly compared with the damping constant Γ of a purely Lorentzian representation.

E. Holden's model

Holden's model (HM) describes the dielectric function with the expressions based on the electronic energy-band structure near critical points and excitonic and Coulomb enhancement effects.[73] It has been applied to a material exhibiting well defined excitonic structure[73] and material where excitonic effects at the band gap E_0 are not resolved.[74,75] The HM equations are similar to the results of Goñi et al.[76] The important advantage of HM is that both the real and imaginary parts of the dielectric function are expressed analytically [Eqs. (A7) and (A12) in Ref. 73]. Unlike expressions proposed by Tanguy,[59–62] HM and the work of Goñi et al.[76] express the optical functions in terms of the simple algebraic functions. Model equations are still rather intricate, but the number of parameters required is small. The important advantage of this model is that accurate determination of the Rydberg energies for both 2D and 3D excitons is possible. However, these parameters (as well as some other parameters related to the structures not well resolved, such as $E_0 + \Delta_0$) need to be determined from fitting the first derivative and they are kept fixed in fitting the dielectric function. Also, applications of this model take into account $E_0, E_0 + \Delta_0, E_1, E_1 + \Delta_1$, and E_2 (single DHO), which correspond to the zinc-blende structure. The dielectric function spectra
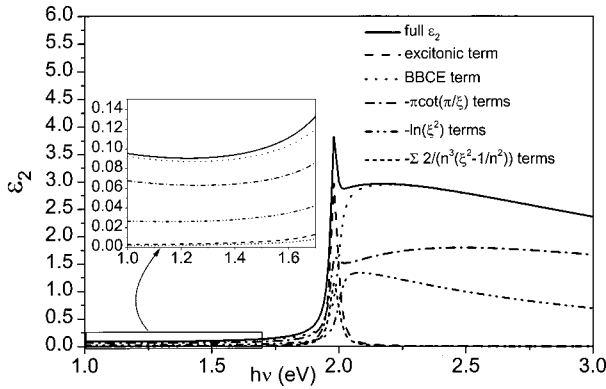
FIG. 4. The contributions of the Holden's model for the E_0 transition Holden's model to the imaginary part of the dielectric function ($E_0=2.0$ eV, $R_0=20$ meV, $A=4$ eV^2, $\Gamma_0=0.020$ meV, and $\Gamma_{ex}=20$ meV).
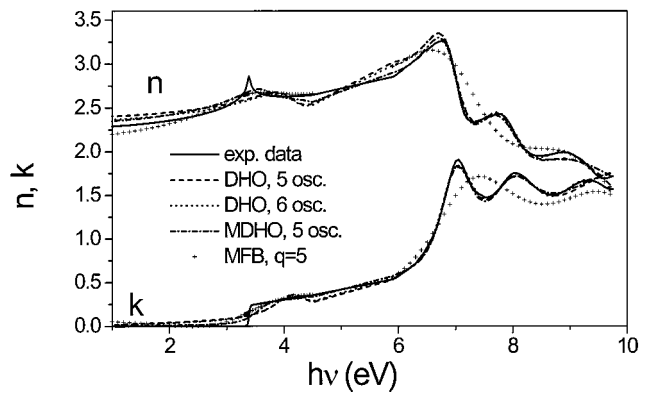

FIG. 5. The real and imaginary part of the index of refraction of GaN. Solid line—experimental data (see Ref. 16) dashed line—DHO with five oscillators, dotted line—DHO with six oscillators, and dash-dot line—modified DHO with adjustable broadening and five oscillators, $+-$ MFB.

of GaN reveals four distinct structures which should correspond to E_0 (3D) and E_{1A}, E_{1B}, E_{1C} (2D) CPs. We have tried to fit the data with expressions corresponding to one 3D+ three 2D structures, or two 3D+ two 2D structures and failed to achieve good agreement with the experimental data above 6 eV (spectral region dominated by $E_{1\beta}$ transitions). Combinations of one 3D term and 4 DHOs or one 3D+ two 2D terms +2 DHOs gave good agreement with the experimental data. This might indicate that further investigation of the nature of $E_{1\beta}$ critical points is needed. There are some important shortcomings of this model which should be noted. Since purely Lorentzian broadening is used, extended absorption tail is evident (see Fig. 4 in Ref. 73). The significant contribution to the ϵ_2 below the band gap represents an important shortcoming of this model. This problem has been avoided in an artificial way by introducing the linear cutoff for the contributions of the higher lying critical points ($E_1, E_1+\Delta_1, E_2$ and indirect gap E_{ind}). Figure 4 shows separate contributions to the ϵ_2 in the range 1–3 eV. Problems stemming from the terms $-\ln(\xi^2)$ and $-\pi \cot(\pi/\xi)$ can be clearly observed. As will be shown in the following, excessive absorption can be reduced if adjustable broadening is used, as predicted by Schubert *et al.*[72] However, the extended absorption tail in this model cannot be fully eliminated. Another shortcoming of Holden's model[73] is that the division by E^2 instead of $(E+i\Gamma)^2$ leads to singularity in $E=0$.

III. RESULTS AND DISCUSSION

The following objective function was employed for the model parameter estimation:

$$E(\boldsymbol{p})=\sum_{i=1}^{i=N_p}\left[\left|\frac{\epsilon_1(\omega_i)-\epsilon_1^{\mathrm{exper}}(\omega_i)}{\epsilon_1^{\mathrm{exper}}(\omega_i)}\right|+\left|\frac{\epsilon_2(\omega_i)-\epsilon_2^{\mathrm{exper}}(\omega_i)}{\epsilon_2^{\mathrm{exper}}(\omega_i)}\right|\right]^2.$$
(21)

where N_p is number of experimental points, $\epsilon_1(\omega_i)$, $\epsilon_2(\omega_i)$ are calculated values of real and imaginary part of the dielectric constant at frequency ω_i, while $\epsilon_1^{\mathrm{exper}}(\omega_i)$, $\epsilon_2^{\mathrm{exper}}(\omega_i)$ are the corresponding experimental values. In the case $\epsilon_2^{\mathrm{exper}}(\omega_i)=0$, $|\epsilon_2(\omega_i)-\epsilon_2^{\mathrm{exper}}(\omega_i)|$ has been considered in

Eq. (21), instead of $|[\epsilon_2(\omega_i)-\epsilon_2^{\mathrm{exper}}(\omega_i)]/\epsilon_2^{\mathrm{exper}}(\omega_i)|$. The objective function was minimized by acceptance probability controlled simulated annealing algorithm with adaptive move-generation procedure, which is described in detail in Ref. 58

Figure 5 shows the real and imaginary part of the index of refraction of GaN. The solid line represents the experimental data,[16] the dashed line denotes the DHO model with five oscillators, the dotted line denotes the DHO model with six oscillators, and the dash-dot line denotes the MDHO model with adjustable broadening and five oscillators, $+-$ MFB. The obtained relative rms errors for the real and imaginary part of the index of refraction, ρ_n and ρ_k, are: $\rho_n=2.3\%$ and $\rho_k=9.2\%$ for the MDHO model, $\rho_n=3.4\%$ and $\rho_k=11.5\%$ for the DHO model (five oscillators), $\rho_n=3.1\%$ and $\rho_k=11.5\%$ for the DHO model (six oscillators), and $\rho_n=5.3\%$ and $\rho_k=10.0\%$ for the MFB. It can be clearly observed that DHO and MDHO models achieve sufficient accuracy in the spectral region above the band gap. However, in the vicinity and below the absorption edge neither of the models shown in Fig. 5 can be considered accurate enough, although the MDHO with five oscillators achieves better results than the conventional DHO models, both for five and six oscillators. MFB ($q=5$, 17 parameters) exhibits the worst agreement with the experimental data. The performance of the MFB in the region above the absorption edge can be improved if more transitions are taken into account. However, in that case the only advantage of this model, i.e., low number of parameters required, would be lost.

Figure 6 shows the real and imaginary part of the index of refraction of GaN. The solid line represents the experimental data,[16] the dashed line denotes MDF, the dotted line denotes the MMDF, the dash-dot line denotes the MCP model. The inset shows the enlarged region around the absorption edge. The obtained relative rms errors for the real and imaginary part of the index of refraction, ρ_n and ρ_k, are: $\rho_n=1.0\%$ and $\rho_k=12.5\%$ for the MDF, $\rho_n=1.0\%$ and $\rho_k=7.4\%$ for the MMDF (five oscillators), and $\rho_n=0.6\%$ and $\rho_k=2.0\%$ for the MCP model. It can be observed that all
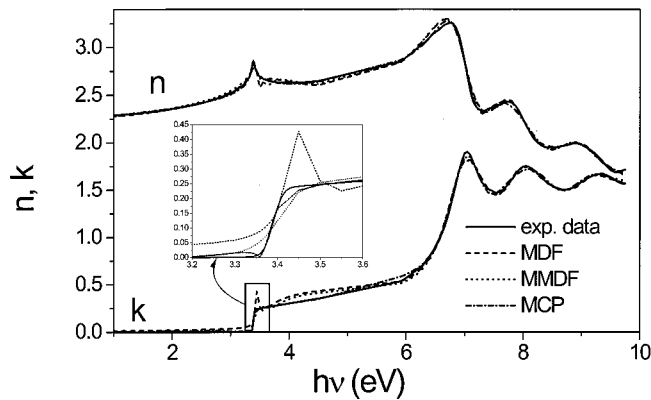
FIG. 6. The real and imaginary part of the index of refraction of GaN. Solid line—experimental data (see Ref. 16) dashed line—MDF, dotted line—modified MDF with adjustable broadening, and dash-dot line—MCP. The inset shows the enlarged region around the absorption edge.
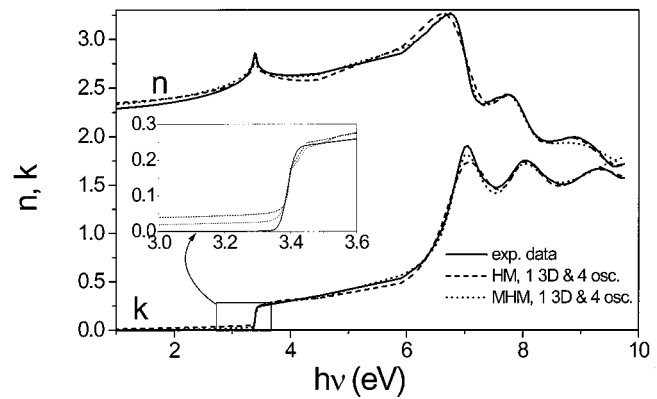

FIG. 7. The real and imaginary part of the index of refraction of GaN. Solid line—experimental data (see Ref. 16) dashed line—HM with one 3D transition and four oscillators, and dotted line—modified HM with adjustable broadening. The inset shows the enlarged region around the absorption edge.

the models achieve good agreement with the experimental data. The best agreement has been accomplished with the MCP model. The accuracy of the MDF and MMDF is lower than that of the MCP in the region around the absorption edge. In order to avoid obtaining unrealistically large values for the exciton binding energy G_0^{3D} we have imposed constraints on this value, which resulted in an obvious excitonic peak in the calculated curves, which is more pronounced in the MDF. The optical functions for GaN in general do not show well resolved excitonic peak at E_0, with the exception of absorption coefficient data of Muth et al.[77] Also, the MDF exhibits extended absorption tail below the band gap E_0, which is inherent to all models with Lorentzian broadening. From Fig. 6 and obtained rms errors, it can be observed that the MMDF achieves better agreement with the experimental data than the MDF. Obtained critical points energies[78] for both the MMDF and MCP are in good agreement with the expected values $E_0 \sim 3.45$ eV,[77] $E_{1A} \sim 7$ eV, $E_{1B} \sim 8$ eV,[5,15,17,47] and $E_{1C} \sim 9$ eV.[5,17,47] Exciton binding energy at the absorption edge is expected to be around 20 meV.[77]

Since Holden's model[73] has been proposed for zinc-blende semiconductors, it is not possible to apply it directly to a hexagonal material, such as GaN. We have investigated several different combinations of 3D and 2D transitions with damped harmonic oscillators for describing higher-lying transitions. Good results have been obtained in two cases: (a) one 3D contribution, two 2D contributions and 2 DHOs, and (b) one 3D contribution and 4 DHOs. As expected, in the latter case excellent agreement with the experimental data can be obtained, since high accuracy can be accomplished with the DHO model above the absorption edge. However, in the region in the vicinity of the band gap and below, conventional Holden's 3D term[73] with Lorentzian broadening exhibits extended absorption tail which hinders the accuracy of this model. In the modified Holden's model (MHM) absorption below the gap can be reduced, but not fully eliminated. Figure 7 shows the real and imaginary part of the index of refraction of GaN. The solid line represents the experimental data,[16] the dashed line denotes HM, the dotted line denotes the MHM. The inset shows the enlarged region around the

absorption edge. The obtained relative rms errors for the real and imaginary part of the index of refraction are: $\rho_n = 1.7\%$ and $\rho_k = 4.2\%$ for HM, $\rho_n = 1.3\%$ and $\rho_k = 3.4\%$ for the MHM. However, in this case it is not possible to estimate positions of the higher-lying critical points (energy of the DHO is not related in a simple way to energy of a critical point[32]) and Rydberg energy of 2D excitons. In order to achieve that it is necessary to describe the dielectric function with one 3D contribution, two 2D contributions and 2 DHOs. Figure 8 shows the real and imaginary part of the index of refraction of GaN. The solid line represents the experimental data,[16] dashed line denotes the HM, dotted line denotes MHM. The inset shows the enlarged region around the absorption edge. The obtained relative rms errors for the real and imaginary part of the index of refraction are: $\rho_n = 2.5\%$ and $\rho_k = 4.8\%$ for HM, $\rho_n = 1.3\%$ and $\rho_k = 2.0\%$ for the MHM. In this case we can also observe excessive absorption below the band gap in the conventional HM, which is reduced in the MHM. Also, with conventional HM we obtain low broadening constant for the transitions at E_{1A} and E_{1B} which results in sharp excitonic peaks absent in the experi-
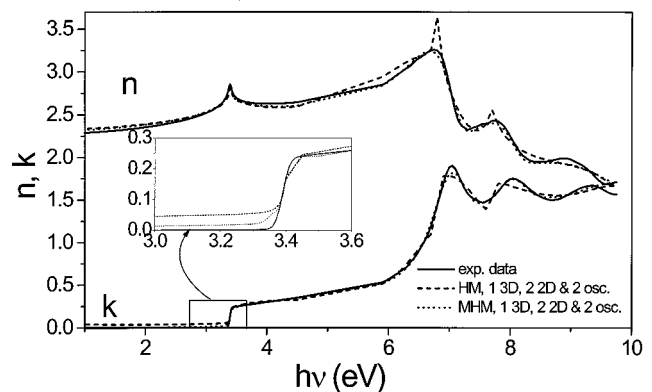

FIG. 8. The real and imaginary part of the index of refraction of GaN. Solid line—experimental data (see Ref. 16) dashed line—HM with one 3D transition, two 2D transitions and two oscillators, dotted line—modified HM with adjustable broadening. The inset shows the enlarged region around the absorption edge.
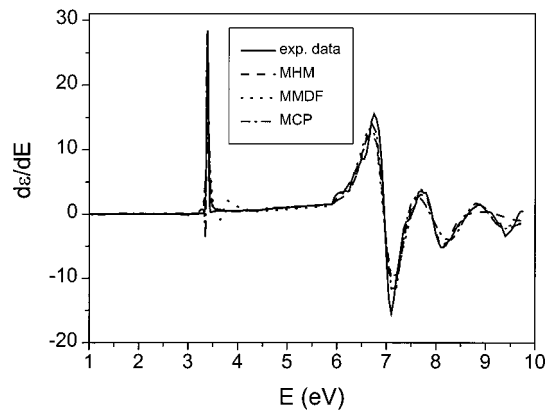
FIG. 9. The first derivative of the imaginary part of the dielectric function of GaN. Solid line—experimental data (see Ref. 16) dashed line—modified MDF, dotted line—modified critical points model, and dash-dot line—modified Holden's model.

mental data. Imposing constraints on this value failed to result in a better fit, since in that case flattened curve with underestimated peaks is obtained. As for the MMDF and MCP, the estimate of the position of critical points is in good agreement with the expected positions.[78] Obtained value for Rydberg energy of 2D excitons is $R_1 = 0.331$ eV. From $R_1 \sim \mu_\perp / \epsilon^2(\infty)$, where $\mu_\perp$ is the reduced effective mass which can be calculated from the effective mass parameters determined by Yeo et al.,[79] and $\epsilon(\infty) = 5.29$[80] we estimate $R_1 = 0.244$ eV which is in agreement with the estimate from the experimental data, considering that all our values are determined by fitting the dielectric function. For more precise estimation of certain parameter values, fitting the derivative(s) of the dielectric function can be considered, possibly over a more narrow spectral range.

To summarize, we have modeled the optical functions of GaN using a variety of semi-empirical models. We have demonstrated that in all cases adjustable broadening needs to be employed instead of the conventional Lorentzian one in order to eliminate extended absorption tail below the band gap. Excellent agreement with the experimental data has been accomplished for the MMDF, MHM, and MCP models. For those models good agreement with the derivatives of the dielectric function can also be achieved, as shown in Fig. 9. The solid line represents the experimental data,[16] the dashed line is the modified MDF, the dotted line is the modified critical points model, and the dash-dot line denotes modified Holden's model. It can be observed that it is justified to treat E_{0A}, E_{0B}, E_{0C} in hexagonal GaN as a single E_0 critical point, since only one peak can be observed in the room temperature spectrum of the first derivative of the dielectric function. The MCP model achieves the best agreement with the dielectric function, while the best agreement with the derivative (obtained by numerical derivation of the dielectric function and not by fitting the derivative of the dielectric function) is obtained by the MHM, since in this case the absorption tail, whose slope is very low, practically has no influence. Small discrepancy around the absorption edge for the MMDF is due to resolved excitonic peak obtained using this model. If no constraint on G_0^{3D} value is imposed, this

feature can be eliminated, but in that case G_0^{3D} can be largely overestimated. Obtained broadening parameters for all three models cannot be directly compared with the conventional Lorentzian broadening. KK consistency of the obtained results has been checked numerically, and satisfactory results have been obtained. It is advisable to check KK consistency numerically when using adjustable broadening modification.[72] Also, it can be recommended to artificially set ϵ_2 to zero in the MCP below E_0 after it reaches 0.001 value to avoid small oscillations which can be present. In the MHM, however, $\epsilon_2 > 0$ values cannot be avoided in such manner, since the absorption tail is decaying very slowly. The MMDF does not suffer from such problems.

IV. CONCLUSION

We have modeled the optical functions of hexagonal GaN in the range from 1 to 10 eV using several different models. The models have been compared in terms of agreement with the experimental data, the intricacy of model equations, the number of parameters required and their physical meaning. Excellent agreement with the experimental data for GaN has been achieved using modified Holden's model with adjustable broadening, modified Adachi's model with adjustable broadening, and modified critical points model. In cases where good agreement with the experimental data has been achieved, broadening function is not purely Lorentzian.

[1] I. Akasaki and H. Amano, J. Electrochem. Soc. **141**, 2266 (1994).
[2] S. Nakamura and G. Fasol, *The Blue Laser Diode: GaN Based Light Emitters and Lasers* (Springer, Berlin, 1997).
[3] Z. Yang and Z. Xu, J. Phys.: Condens. Matter **8**, 8303 (1996).
[4] Z. Yang and Z. Xu, Phys. Rev. B **54**, 17577 (1996).
[5] W. R. Lambrecht, B. Segall, J. Rife, W. R. Hunter, and D. K. Wickenden, Phys. Rev. B **51**, 13516 (1995).
[6] J. L. P. Hughes, J. Wang, and J. Sipe, Phys. Rev. B **55**, 13630 (1997).
[7] Y. N. Xu and W. Y. Ching, Phys. Rev. B **48**, 4335 (1993).
[8] L. H. Benedict, E. L. Shirley, and R. B. Bohn, Phys. Rev. B **57**, R9385 (1998).
[9] L. H. Benedict, E. L. Shirley, and R. B. Bohn, Phys. Rev. Lett. **80**, 4514 (1998).
[10] M. Rohlfing and S. G. Louie, Phys. Rev. Lett. **81**, 2312 (1998).
[11] S. Albrecht, L. Reining, R. Del Sole, and G. Onida, Phys. Rev. Lett. **80**, 4510 (1998).
[12] L. H. Benedict and E. L. Shirley, Phys. Rev. B **59**, 5441 (1999).
[13] M. Cardona, L. F. Lastras-Martinez, and D. E. Aspnes, Phys. Rev. Lett. **83**, 3970 (1999).
[14] S. Albrecht, L. Reining, G. Onida, V. Olevano, and R. Del Sole, Phys. Rev. Lett. **83**, 3971 (1999).
[15] T. Whetkamp et al., Thin Solid Films **313–314**, 745 (1998).
[16] R. Goldhahn (private communication).
[17] S. Logothetidis, J. Petalas, M. Cardona, and T. D. Moustakas, Phys. Rev. B **50**, 18 017 (1994).
[18] T. Kawashima, H. Yoshikawa, S. Adachi, S. Fuke, and K. Ohtsuka, J. Appl. Phys. **82**, 3528 (1997).
[19] D. Brunner, H. Angerer, E. Bustarret, F. Freudenberg, R. Höpler, R. Dimitrov, O. Ambacher, and M. Stutzmann, J. Appl. Phys. **82**, 5090 (1997).
[20] D. E. Aspnes and A. A. Studna, Phys. Rev. B **27**, 985 (1983).

[21] S. Shokhovets, R. Goldhahn, G. Gobsch, T. S. Cheng, C. T. Foxon, G. D. Kipshidze, and Wo. Richter, J. Appl. Phys. **86**, 2602 (1999).

[22] R. Goldhahn *et al.*, Phys. Status Solidi A **177**, 107 (2000).

[23] T. Takeuchi, H. Takeuchi, S. Sota, H. Amano, and I. Akasaki, Jpn. J. Appl. Phys., Part 2 **36**, L177 (1997).

[24] J. N. Kuznia, M. Asif Khan, D. T. Olson, R. Kaplan, and J. Freitas, J. Appl. Phys. **73**, 4700 (1993).

[25] N. V. Edwards, M. D. Bremser, T. W. Weeks, Jr., R. S. Kern, R. F. Davis, and D. E. Aspnes, Appl. Phys. Lett. **69**, 2065 (1996).

[26] R. M. Bueno, J. F. Trigo, J. M. Martinez-Durat, E. Elizalde, and J. M. Sanz, J. Vac. Sci. Technol. A **13**, 2378 (1995).

[27] B. Harbecke, Appl. Phys. B: Photophys. Laser Chem. **39**, 165 (1986).

[28] L. Vriens and W. Rippens, Appl. Opt. **22**, 4105 (1983).

[29] Y. H. Yang and J. R. Abelson, J. Vac. Sci. Technol. A **13**, 1145 (1995).

[30] M. J. Bergmann, Ü. Özgur, H. C. Casey, Jr., H. O. Everitt, and J. F. Muth, Appl. Phys. Lett. **75**, 67 (1999).

[31] J. Barth, R. L. Johnson, and M. Cardona, in *Handbook of Optical Functions of Solids II*, edited by E. D. Palik (Academic, San Diego, 1991), pp. 213–246.

[32] C. C. Kim, J. W. Garland, H. Abad, and P. M. Raccah, Phys. Rev. B **45**, 11749 (1992).

[33] M. Erman, J. B. Theeten, P. Chambon, S. M. Kelso, and D. E. Aspnes, J. Appl. Phys. **56**, 2664 (1984).

[34] F. L. Terry, Jr., J. Appl. Phys. **70**, 409 (1991).

[35] A. B. Djurišić and E. H. Li, Opt. Commun. **157**, 72 (1998).

[36] G. Yu, G. Wang, H. Ishikawa, M. Umeno, T. Soga, T. Egawa, J. Watanabe, and T. Jimbo, Appl. Phys. Lett. **70**, 3209 (1997).

[37] M. A. Vidal, G. Ramirez-Flores, H. Navarro-Contreras, A. Lastras-Martinez, R. C. Powell, and J. E. Greene, Appl. Phys. Lett. **68**, 441 (1996).

[38] A. R. Forouhi and I. Bloomer, in *Handbook of Optical Constants of Solids II*, edited by E. D. Palik (Academic, San Diego, 1991), pp. 151–175.

[39] A. R. Forouhi and I. Bloomer, Phys. Rev. B **38**, 1865 (1988).

[40] Y. F. Chen, C. M. Kwei, and C. J. Tung, Phys. Rev. B **48**, 4373 (1993).

[41] W. A. McGahan, T. Makovicka, J. Hale, and J. A. Woollam, Thin Solid Films **253**, 57 (1994).

[42] G. E. Jellison, Jr. and F. A. Modine, Appl. Phys. Lett. **69**, 371 (1996).

[43] M. Cardona, *Modulation Spectroscopy* (Academic, New York, 1969), pp. 15–23.

[44] P. Y. Yu and M. Cardona, *Fundamentals of Semiconductors* (Springer, Berlin, 1998).

[45] J. W. Garland, C. C. Kim, H. Abad, and P. M. Raccah, Thin Solid Films **233**, 148 (1992).

[46] J. W. Garland, C. Kim, H. Abad, and P. M. Raccah, Phys. Rev. B **41**, 7602 (1990).

[47] J. Petalas, S. Logothetidis, S. Boultadakis, M. Alouani, and J. M. Wills, Phys. Rev. B **52**, 8082 (1995).

[48] S. Adachi, Phys. Rev. B **41**, 3504 (1990).

[49] T. Kawashima, S. Adachi, H. Miyake, and K. Sugiyama, J. Appl. Phys. **84**, 5202 (1998).

[50] S. Ozaki and S. Adachi, J. Appl. Phys. **78**, 3380 (1995).

[51] C. W. Higginbotham, M. Cardona, and F. H. Pollak, Phys. Rev. **184**, 821 (1969).

[52] D. W. Jenkins, J. Appl. Phys. **68**, 1848 (1990).

[53] R. J. Deri and M. A. Emanuel, J. Appl. Phys. **74**, 3435 (1993).

[54] J. Zheng, C.-H. Lin, and C. H. Kuo, J. Appl. Phys. **82**, 792 (1997).

[55] A. D. Rakić and M. L. Majewski, J. Appl. Phys. **80**, 5509 (1996).

[56] A. B. Djurišić and E. H. Li, Appl. Phys. Lett. **73**, 868 (1998).

[57] A. B. Djurišić and E. H. Li, J. Appl. Phys. **85**, 2848 (1999).

[58] A. B. Djurišić, A. D. Rakić, and J. M. Elazar, Phys. Rev. E **55**, 4797 (1997).

[59] C. Tanguy, IEEE J. Quantum Electron. **32**, 1746 (1996).

[60] C. Tanguy, Phys. Rev. Lett. **75**, 4090 (1995).

[61] C. Tanguy, Phys. Rev. B **60**, 10660 (1999).

[62] B. Sermage, S. Petiot, C. Tanguy, Le Si Dang, and R. André, J. Appl. Phys. **83**, 7903 (1998).

[63] J. W. Garland, H. Abad, M. Viccaro, and P. M. Raccah, Appl. Phys. Lett. **52**, 1176 (1998).

[64] A. Franke, A. Stendal, O. Stenzel, and C. von Borczyskowski, Pure Appl. Opt. **5**, 845 (1996).

[65] R. Brandel and D. Boreman, J. Appl. Phys. **71**, 1 (1992).

[66] C. C. Kim, J. W. Garland, H. Abad, and P. M. Raccah, Phys. Rev. B **47**, 1876 (1993).

[67] C. C. Kim and S. Sivananthan, J. Appl. Phys. **78**, 4003 (1995).

[68] C. C. Kim and S. Sivananthan, Phys. Rev. B **53**, 1475 (1996).

[69] D. E. Aspnes, Sol. Energy Mater. Sol. Cells **32**, 413 (1994).

[70] D. E. Aspnes, Surf. Sci. **135**, 284 (1983).

[71] E. C. Titchmarsh, *Introduction to the Theory of Fourier Integrals* (Oxford University Press, Oxford, 1950).

[72] M. Schubert, J. A. Woollam, G. Leibiger, B. Rheinländer, I. Pietzonka, T. Saß, and V. Gottschalch, J. Appl. Phys. **86**, 2025 (1999).

[73] T. Holden, P. Ram, F. H. Pollak, J. L. Freeouf, B. X. Yang, and M. C. Tamargo, Phys. Rev. B **56**, 4037 (1997).

[74] K. Wei, F. H. Pollak, J. L. Freeouf, D. Shvydka, and A. D. Compaan, J. Appl. Phys. **85**, 7418 (1999).

[75] F. H. Pollak, M. Muñoz, T. Holden, K. Wei, and V. M. Asnin, Phys. Status Solidi B **215**, 33 (1999).

[76] A. R. Goñi, A. Cantarero, K. Syassen, and M. Cardona, Phys. Rev. B **41**, 10111 (1990).

[77] J. F. Muth, J. H. Lee, I. K. Shmagin, R. M. Kolbas, H. C. Casey, Jr., B. P. Keller, U. K. Mishra, and S. P. DenBaars, Appl. Phys. Lett. **71**, 2572 (1997).

[78] The list of all model parameters is available upon e-mail request.

[79] Y. C. Yeo, T. C. Chong, and M. F. Li, J. Appl. Phys. **83**, 1429 (1998).

[80] T. Azuhata, T. Sota, K. Suzuki, and S. Nakamura, J. Phys.: Condens. Matter **7**, L129 (1995).